

Evolutionary Algorithm Tuned PID controller based NOSLLC-SC converter for PV Application

V. Mahesh and S.Saravanan

¹EEE Department, Nalla Malla Reddy Engineering College, Hyderabad, Telangana, India.

E-mail: maheshv81@gmail.com

²EEE Department, B.V.Raju Institute of Technology, Narsapur, Telangana, India.

Abstract

The Photovoltaic (PV) system is more efficient and inherently safe when compared to other power generating technologies with larger life. But PV energy source failed by achieving efficient power generation and gets disturbed over changing atmospheric circumstances. Hence, to overcome the above-mentioned drawback, an efficient evolutionary algorithm tuned PID controller based Negative Output Super-Lift Luo Converter (NOSLLC) using Sheppard-Taylor (S-T) topology has been developed for PV applications. This proposed converter produces efficient energy, higher output voltage with minimum duty ratio, and lower voltage (0.0187) with low settling time (0.02s). In addition to that Gey Wolf optimization algorithm operates within low oscillation of power under stable and varying conditions. Thus, the proposed system enhances maximum power generation under low radiation and various atmospheric conditions.

Keywords: NOSLLC, Sheppard -Taylor's topology, Gey Wolf Algorithm, Photovoltaic Cell, Renewable energy.

1. Introduction

The Photovoltaic system converts light energy into electrical direct current using photo electric effect. Even though this system is more efficient it has some demerits like high capital cost and produces low efficiency. To improve the overall function of the PV system it should be merged with the converter. Generally, the DC-DC converter employs a significant role in the extraction of electrical power. But DC-DC converter gives less output power density in photovoltaic applications due to variation of sunlight. The traditional DC-DC converter, Super Lift LUO converter can be refreshed to improve power [1]. Super Lift LUO converter is the modified model of the DC-DC converter, which has various merits like high efficiency, high power density, high output with low repulsion, compact and simple [2]. The Super Lift LUO converter is further classified into two classes, namely POESLLC and a NOSLLC [3]. This system concentrates more on NOSLLC based on Sheppard-Taylor topology to maximize the power generation. These converters implement voltage gain in terms of arithmetic progress whereas DC-DC converters implement in geometric progress. Some of the merits of NOSLLC are high-voltage gain, high efficiency, decreased ripple current and voltage [4]. These NOSLLC are broadly utilized in computer applications, industrial applications, and in high voltage-voltage projects. This technique generally raises the transfer of voltage in the step by step expansion of symmetrical progression [5]. Sheppard -Taylor's topology is commonly used in the regulation of energy in a photovoltaic system. It can regulate efficiently and is also capable of regulating even in varying load conditions [6]. This technique reduces ripples and is suited for power factor correction applications. In general, the S-T converter consists of two switches and four diodes that work based on synchronization. Further, the synchronization lack between the two switches does not lead to a converter break down. The only demerits of Sheppard -Taylor topology is actual ON/OFF power loss occurs while higher frequency operations [7].

To obtain extreme power extraction, Maximum power point tracking (MPPT) algorithm can be used. The MPPT techniques like Perturbation and observation, Incremental conductance, Fuzzy logic control methods can be utilized in the generation of energy in the photovoltaic system. Fuzzy Logic control MPPT technique, which is an advanced method of VLSI technology was widely used in the photovoltaic module. This method is used in tracking and extracting maximum energy in solar applications [8]. The Perturbation and Observation (P&O) procedure operates by occasionally

perturbing the cell output voltage and relating the PV terminal power with the earlier perturbation cycle. By incrementing the PV operating voltage, it is moved toward the optimum point of the converter. But in this technique, there is a difficulty in drift effect [9]. A drawback of this algorithm is that the cell output voltage is perturbed every MPPT cycle; so, the terminal power starts oscillating when it reaches MPP, which results in a loss in power in the PV system. This system is accurate in stable and gradually changing atmospheric conditions but not under the quickly changing condition.

The Incremental conductance MPPT method gives the best consequences during quickly altering atmospheric conditions and utilized as a part of the P&O algorithm in extreme energy generation of the photovoltaic system [10]. This method was decided to work with more efficiency in randomly created condition; it is negative in left and positive on right [11]. When MPPT has been gotten once the function of PV array is sustained at this point and perturbation stopped except an alteration in current is observed. At this time, the algorithm decrement or increment the voltage in PV array to trace MPP. The increment size determines how fast MPP is tracked. Generally, the MPP is traced by relating the impedance of the PV cell with the actual impedance of the converter. But these techniques are not able to produce maximum energy and leads to reduced efficiency in low radiation condition and various atmospheric conditions. To overcome these demerits, Artificial Neural Network (ANN) MPPT technique is used. ANN-based controller MPPT technique is more efficient, provides a faster response and error in oscillation can be reduced [12]. In [13], the proposed method provides duty cycle for various atmospheric condition, so the input and output data's nonlinear relationship is mapped faster. Since the utmost PV module has characteristics dissimilar, this method should be trained for the PV array with which it will be used and these characteristics also vary with time, implying that the ANN has to be periodically trained to give accurate MPPT.

GWO technique is a comparatively novel, vigorous and influential optimization technique designed by Seyedali in 2014. In a multi-area system, Grey Wolf Optimization provides satisfactory damping performance under load demand and step disturbances [14]. In [15] proposed a Sorting Genetic Algorithm-II technique is employed in TCSC centered stabilizer geared towards tuning the PID controller to get better damping with the least cost. Depending upon various load demands of a single bus system, a fuzzy logic-based UPFC drew up towards improving transient stability performance [16]. To enhance the efficiency of the solar module, it is necessary to link a converter with the PID controller system. The object of this paper is to combine Negative Output Super-Lift Luo Converter (NOSLLC) based on Sheppard-Taylor topology with Grey Wolf Optimization tuned PID Controller to achieve maximum power generation with high efficiency even in changing environmental conditions with optimal duty cycle within a limited time convergent.

This paper is further arranged as follows. Section 2 describes the proposed system, and further sub-section is divided into three parts which explain the modeling of PV cell, modeling of NOSLLC based on Sheppard-Taylor topology and GWO tuned PID controller. Section 3 shows the simulation results and discussion and Section 4 gives the conclusion of this paper.

2. Evolutionary Algorithm Tuned Pid Controlled Converter Model

The Evolutional algorithm tuned PID controlled NOSLLC-SC converter has been given in Fig 1. The Current and voltage are monitored with respect to the duty ratio of the switching gate pulse of NOSLLC.

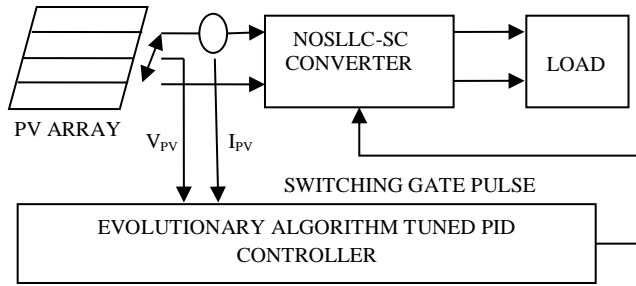


Fig 1. Evolutionary Algorithm Tuned PID Controlled NOSLLC-SC Converter Model

The PV array is linked to the load using the NOSLLC-SC converter. From the PV Array, the maximum voltage and current are monitored by the Grey Wolf Optimization tuned PID controller. Scaled weights lead to time convergent and cause an inaccurate pulse value, hence to overcome this Grey Wolf Optimization has been used. The converter then produces a constant output voltage with a low oscillation error. Hence, the proposed converter is drift-free and generates maximum energy with high efficiency in low radiation conditions and various atmospheric conditions within a small period of time with an optimal solution.

2.1. Modeling of Photovoltaic Cell

In the photovoltaic scheme, the light energy is converted into electrical direct current using the photovoltaic effect. The photovoltaic cell is a nonlinear device, which varies with respect to current and voltage. A single photovoltaic cell can generate only a few amounts of electric power. Hence, numerous photovoltaic cells are connected together to generate the desired amount of power. These cells are classically constructed based on a p-n junction diode. The equivalent circuit of the photovoltaic cell has been shown in Fig.2. In this equivalent circuit, the shunt resistor is utilized to reduce the current leakage.

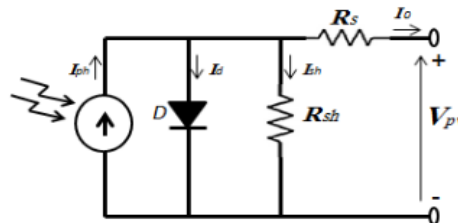


Fig 2. Equivalent circuit of Photovoltaic module

The output current of the photovoltaic module can be determined using Kirchoff's current law (KCL), it is expressed as,

$$I_o = I_{ph} - I_d - I_{sh} \quad (1)$$

Where, I_{ph} is the output current in the photovoltaic cell (A), I_d is the current across the diode (A), I_{sh} is shunt resistor current (A). The voltage-current performance equation of the photovoltaic module is expressed below,

$$I_o = N_p I_{ph} - N_p I_{rs} \left[e^{\frac{q(V+R_s I_o)}{A k T N_s}} - 1 \right] - N_p \frac{q(V+R_s I_o)}{N_s R_{sh}} \quad (2)$$

Where, I_{rs} is the reverse saturation current of photovoltaic array, V is the output voltage of photovoltaic array, A is the ideal constant of diode, T is the operating temperature, q is the charge of electrons ($1.60217646 \times 10C$), k is the Boltzmann constant, and R_s, R_p are shunt and series

resistors of the cell. The relation between solar irradiation and extracted solar current is expressed as,

$$I_{ph} = \frac{G}{1000} (I_{sc} + K_i(T - T_r)) \quad (3)$$

Here, I_{sc} represent the short circuit current in PV cell, G is Solar irradiation in W/m^2 , T_r represent the reference temperature of the photovoltaic cell, K_i is the temperature coefficient of short circuit current.

2.2 Modelling of Topologized NOSLLC based on Sheppard-Taylor(S-T)

The NOSLLC based on S-T topology has been represented in Fig 3. In order to fix the capacitive current constant, large values are chosen for L , C_2 , and C_3 . It has three modes of operation.

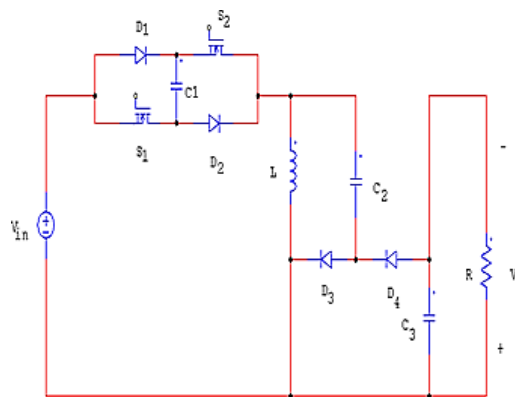


Fig 3. NOSLLC based on Sheppard-Taylor topology.

Mode 1: The mode 1 operation has been depicted in Fig 4. When the switches S_1 and S_2 are closed, the capacitor C_1 gets de-energized, the diodes D_1 , D_2 , D_4 are open and D_3 is closed. The inductor current increases linearly as $V_{in} + V_{C1}$ increases. The input source and C_1 dispense energy to L . Initially at mode 1, the voltage in C_1 is $V_{in} - V_l$, thus the energy in C_1 is $C_1(V_{in} - V_l)^2/2$.

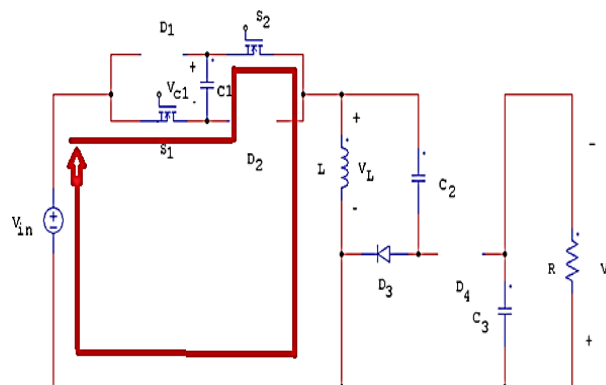


Fig 4. Mode 1 operation.

When the switches S_1 and S_2 are closed, the output voltage V_l is obtained by using Kirchhoff's current law, it is described as,

$$V_l = V_{in} + V_{C1} \quad (4)$$

$$\frac{dI_l}{dT} = \frac{V_{in} + V_{C1}}{L} \quad (5)$$

When $\frac{dI_l}{dT}$ is positive, then the current will be linearly increased and it is expressed as,

$$(\Delta I_l)_{closed} = \left(\frac{V_{in} + V_{c1}}{L} \right) dT \quad (6)$$

Mode 2: When the switches S_1 and S_2 are open, D_3 is closed and D_4 is open while V_{c1} is less than V_0 . C_1 is energized to help the source and inductor through D_1 and D_2 the inductor current I_l falls. Fig 5 shows the Mode 2 operation.

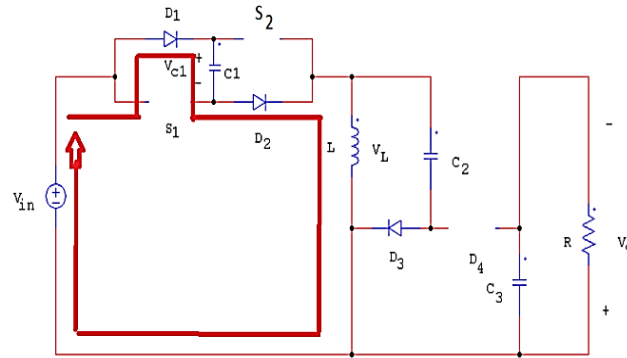


Fig 5. Mode 2 operation.

The inductor voltage is given by,

$$V_l = V_{in} - V_{c1} \quad (7)$$

$$\frac{dI_l}{dT} = \frac{V_{in} - V_{c1}}{L}$$

When $\frac{dI_l}{dT}$ is negative then there will be a linear increment in current and it is expressed by,

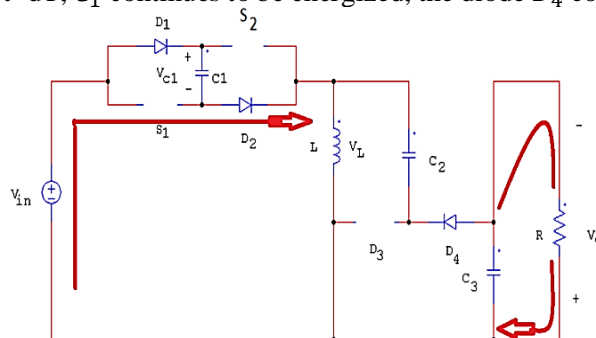
$$(\Delta I_l)_{open} = \left(\frac{V_{in} - V_{c1}}{L} \right) (1 - dT) \quad (8)$$

In steady-state operation the net charge in I_l is null. Hence from equation (3) and (4), I_l can be expressed as,

$$\left(\frac{V_{in} + V_{c1}}{L} \right) dT + \left(\frac{V_{in} - V_{c1}}{L} \right) (1 - dT) = 0$$

$$V_{c1} = \frac{V_{in}}{(1-2d)} \quad (9)$$

Mode 3: The mode 3 operation has been shown in Fig 6. The switches S_1 and S_2 are open and D_4 is closed, V_{c3} drops due to freewheeling. At $t=dT$, C_1 continues to be energized, the diode D_4 conducts



when $V_{c1} = V_0$ and V_{c1} is clamped at V_0 .

Fig 6. Mode 3 operation.

At $t=dT$,

$$V_{c1}(dT) = \frac{-1}{C_1} I_l dT + V_{c1}(0) \quad (10)$$

At $t = d_1 T$,

$$V_{c1}(d_1 T) = \frac{1}{C_1} I_l (d_1 - d) T + V_{c1}(dT) \quad (11)$$

Using equation (6) and (7),

$$V_{c1}(d_1 T) = \frac{1}{C_1} I_l (d_1 - 2d) T + V_{c1}(0) \quad (12)$$

Similarly,

$$V_{c3}(d_1 T) = \frac{-1}{C_3} I_0 d_1 T + V_{c3}(0) \quad (13)$$

Consider $V_{c1} = V_{c3}$, to find d_1 value,

$$d_1 = V_{c1} = \frac{V_{in}}{(1-2d)} \quad (14)$$

2.3 State Space Averaged Modelling of NOSLLC Based On ST:

As there are two capacitors in NOSLLC, with $V_{c2} = V_{in}, V_0$ alone can be chosen as a state-space variable. Similarly, with the inductor current I_{l1} entire space variables of NOSLLC based on S-T can be chosen as I_l, V_0, x_1 and x_2 from (11), (12), and (13), the modeling of NOSLLC based on S-T is given by (14). Using equations (11), (12), and (13), the modeling of the NOSLLC based on S-T may be written as,

$$\begin{bmatrix} \dot{I}_l \\ \dot{V}_0 \end{bmatrix} = \begin{bmatrix} 0 & -\frac{1-d}{L} \\ \frac{1-d}{C_3} & -\frac{1}{RC_3} \end{bmatrix} \begin{bmatrix} I_l \\ V_0 \end{bmatrix} + \begin{bmatrix} 1 \\ 0 \end{bmatrix} V_{in} \quad (18)$$

2.4 GWO based PID controller

GWO technique is a comparatively novel, vigorous and influential optimization technique designed by Seyedali in 2014. Here GWO technique utilized to adjust the PID control for automatic gain control (AGC) of an interrelated system. The block diagram model for GWO based PID controller as shown in Fig 7. The performance index (ζ) can be represented as,

$$\zeta = \int_0^{\infty} (ACE)^2 dt \quad (19)$$

Minimize ζ focused towards:

$$K_P^{minim} \leq K_P \leq K_P^{maxim}$$

$$K_I^{minim} \leq K_I \leq K_I^{maxim}$$

$$K_D^{minim} \leq K_D \leq K_D^{maxim}$$

The above-mentioned controller parameters $K_P = 3.2965$, $K_I = 2.9862$, and $K_D = 2.3334$ has been chosen for this PID controller. To improve the productivity of the solar-powered module it is

important to connect a control strategy in this framework. GWO tuned PID Controller is utilized in the photovoltaic framework to extricate the most extreme power result. The power injection in terms of voltage and power angle is given by,

$$P_{real} - jQ_{reactive} = \bar{V}_r^* I_{line} = \bar{V}_r^* \left(\frac{\bar{V}_s + \bar{V}_{se} - \bar{V}_r}{j(X)} \right) \quad (20)$$

$$\bar{V}_{se} = |V| \angle (\delta_s - \phi_{se}) \quad (21)$$

V_{se} represents series voltage magnitude, θ_{se} represents phase angle towards series voltage.

Regulation of PID controllers towards AGC through GWO algorithm gives better system performance. For an abrupt transform in load require the output of Redox Flow Batteries be given as,

$$\Delta P_R = \left[\frac{K_R}{1 + sT_R} \right] \Delta f(s) \quad (22)$$

K_R is the gain and T_R is the time constant of Redox Flow Batteries expressed as sec. Thus, the proposed framework is connecting NOSSLC dependent on S-T topology and GWO based PID controller.

The Grey Wolf Optimization algorithm deals with finding the best response to an issue from an accumulation of feasible options. Generally, the issue of streamlining is defined as an issue of minimization, where a mistake that relies upon the arrangement is endeavoured to be limited: the ideal arrangement has the base blunder. Distinctive enhancement procedures are actualized in various zones, for example, mechanics, financial matters and designing, and as the multifaceted nature and amount of data included expands, progressively successful techniques are required to settle advancement issues. There are several iterations in the GWO algorithm. It solves a feasibility issue in each iteration, namely finding any solution that meets the following requirements,

$$\begin{aligned} \langle c, k \rangle_{S^n} &\leq t \\ \langle A_k, X \rangle_{S^n} &\leq b_k, \quad k = 1, \dots, m \\ X &\geq 0 \end{aligned} \quad (23)$$

Each iteration, a different threshold t is selected and the algorithm either outputs a solution X such that and other limitations are also satisfied or indicates that there is no such solution.

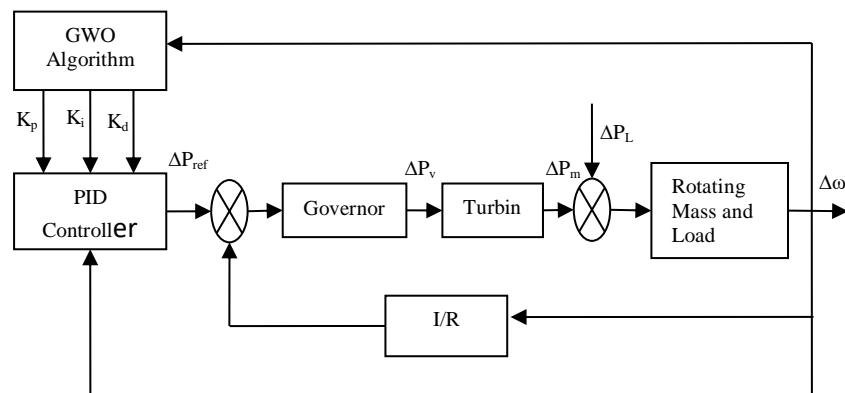


Fig 7. Model of GWO tuned PID Controller

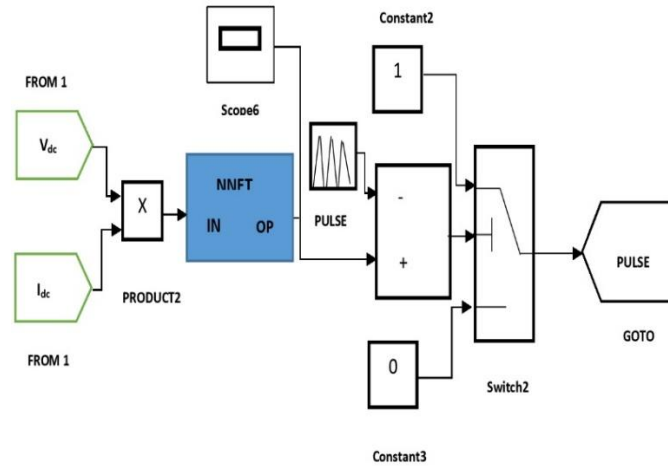


Fig 8. GWO based PID controller Simulink Model.

Fig 8. shows the GWO based PID controller Simulink model. This method is more efficient, fast response and error in oscillation can be reduced. The method provides a lesser duty cycle for various atmospheric conditions, so the input and output data’s nonlinear relationship is mapped faster. The GWO method operates in two stages: the online stage and offline stage. In the offline stage, the neural parameters are trained to determine the ideal neural network controller whereas in the online stage the found optimal neural network controller to trace extreme power in the PV module. The training of this system is given by using an incremental conductance procedure.

3. SIMULATION AND DISCUSSION

To inquire about the performance of the Photovoltaic system using the NOSLLC S-T topology based on the GWO algorithm is simulated by utilizing MATLAB Simulink. Specifications of NOSLLC based on S-T listed are in table 1.

Table.1: Specifications of NOSLLC based on S-T.

Parameters	Value
Input voltage (V_{in})	25V
Output voltage (V_0)	745.2
Inductor (L)	45 μ H
Capacitor (C_1, C_2, C_3)	25 μ F, 45 μ F, 100 μ F
Switching frequency (F_s)	50KHz
Load (R)	100 Ω
Average output current (I_0)	15.86A
Duty ratio (D)	0.51
Peak to peak capacitor ripple (ΔV_0)	-0.2V

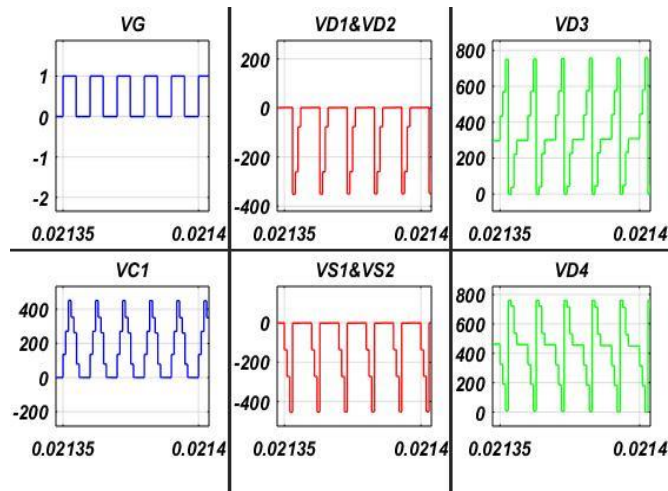


Fig 9. Simulation model of NOSLLC based on S-T with GWO evolutionary algorithm.

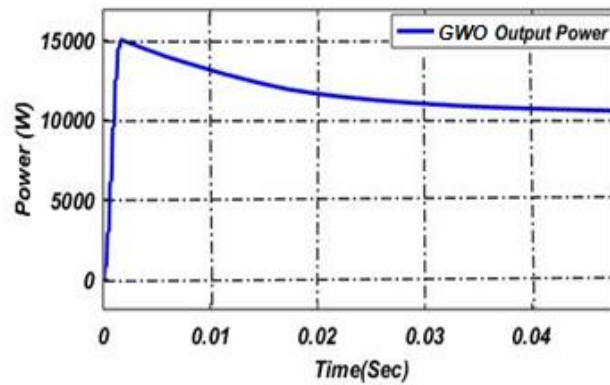


Fig 10. Output Power.

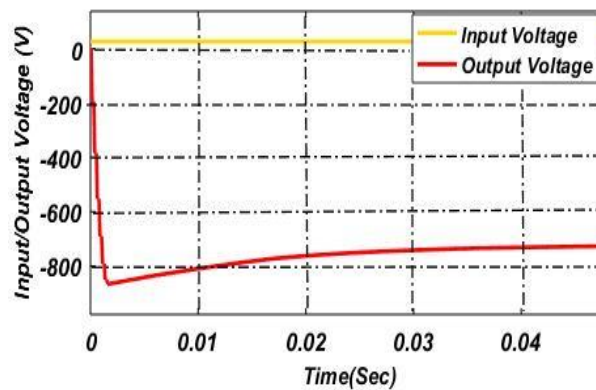


Fig 11. Comparison of input and output voltage.

This portion describes the simulation results of NOSLLC based on S-T topology with GWO algorithm in the photovoltaic system. The converter specification is shown in table 1. Fig 9, Shows the Simulation model of evolutionary algorithm tuned PID controller based Negative Output Super-Lift Luo Converter (NOSLLC) using Sheppard-Taylor (S-T) topology. In this fig, few parameters such as the gate voltage of the switches V_G , the voltage across capacitor the V_{C1} , voltage across the diodes V_{D1} and V_{D2} , the voltage across the switches V_{S1} and V_{S2} , Voltages across the diodes V_{D3} and V_{D4} has been displayed. Figure.10 displays simulated output power waveform in the proposed system with

maximum power 10400W. Figure.11, represents the comparison between the input and output voltage. The input voltage specified to 25V and output voltage produces maximum voltage 721V. From the figure, it is clear that the settling time of the proposed work is very low compared to other methods (0.02s). Thus, it is proven that this system is more efficient and generates maximum energy with high efficiency compared to other techniques.

Table.2: Performance of the NOSLLC based on S-T with Optimised ANN MPPT controller for various input voltage.

Solar Irradiance	NOSLLC based on S-T topology with GWO tuned PID controller			
400 W/m ²	Input PV Voltage (V)	Output PV Voltage (V)	Output PV Current (A)	Power (W)
	20	-542.88	-12.24	7526.5
	25	-721.2	-13.36	8839.1
	30	-754.02	-15.24	11288.7

The table.2 summarizes the performance of the NOSLLC based on S-T with GWO tuned PID controller for various input voltage. From this table, it is clearly represented that NOSLLC based on S-T topology with GWO tuned PID controller in the photovoltaic system produces maximum power with higher efficiency.

4. Conclusion

The performance and the simulation of the NOSLLC based on S-T topology with GWO tuned PID controller has been simulated using MATLAB/Simulink software. The optimized evolutionary algorithm configuration is simple, provides low computational loss, less irradiance, doesn't require any temperature sensors and takes less time while training as well as while testing to obtain an optimal solution. The Simulation result clearly shows that the proposed model has a capacity of extracting maximum power in a range of 11288.7W and operating with high efficiency and reduces voltage ripples (0.0187) with low settling time (0.02s) when compared to other control methods like partial integral controller, Perturbation and observation, Incremental conductance, Fuzzy logic control methods. Therefore, our model achieves a fast and time convergent optimal solution within maximum power extraction and reduced voltage repletion.

Reference

- [1] V. Chamundeeswari & Dr. R. Seyezhai, "Analysis and Experimentation of PV Based NOSLC", IJERT International, Volume 3, 2015.
- [2] Sara Allahabadi, Hossein Iman-Eini and Shahrokh Farhangi, "Neural Network-based Maximum Power Point Tracking Technique for PV Arrays in Mobile Applications", 10th International PEDSTC, February 2019.
- [3] K. Prasanna, Dr. D. Kirubakaran, J. Rahul Kumar, J.A. Rudhran, "Implementation of Positive Output Super Lift Luo Converter for Photovoltaic System", IRJET, December 2019.
- [4] Sabir Messalti, Abd Ghani Harrag, Abd Elhamid Loukriz, "A New Neural Networks MPPT controller for PV Systems", 6th IREC, 2015.
- [5] Razieh Khanaki, M.A.M. Radzi, M. HamiruceMarhaban, "Comparison of ANN and P&O MPPT Methods for PV Applications under Changing Solar Irradiation", IEEE-CEAT, 2013.
- [6] Adi Kurniawan, Eko Haryanto, A.A. Masroeri, "A Neural Network Based Maximum Power Point Tracker with KY Converter for Photovoltaic System on A Moving Vehicle", Int'l Conf. on Advanced Mechatronics, Intelligent Manufacture, and Industrial Automation, 2015.
- [7] Sarthak Jain, Anant Vaibhav, and Lovely Goyal, "Comparative Analysis of MPPT Techniques for PV in Domestic Applications", Annual Conference of the IEEE, 2014.

- [8] Vinay P, Manju Ann Mathews, “Modelling and Analysis of Artificial Intelligence Based MPPT Techniques for PV Applications”, ICAGE, December 2014.
- [9] A. Deepa, Dr. K. Sathish Kumar, “Novel Super Lift Luo-Converter Based on Sheppard-Taylor topology”, Journal of Electrical Engineering.
- [10] Amirtharaj S, Dr.Premalatha L, “Design of an Efficient Positive Output Self-Lift and Negative Output Self-Lift Luo Converters using Drift Free Technique for Photovoltaic Applications”, 1st International Conference on Power Engineering, Computing and Control, March 2017.
- [11] Ankita Arora, Purna Gaur, “Comparison ANN and ANFIS based MPPT Controller for grid-connected PV Systems”, IEEE INDICON, 2015.
- [12] Jyothy Lakshmi P.N, Dr. M R Sindhu, “An Artificial Neural Network Based MPPT Algorithm for Solar PV System”, Annual Conference of the IEEE, 2018.
- [13] Kingston Stanley, P., Sanjeevi Gandhi, A., & Abraham Chandy, D. (2020). Real time control of dissolved oxygen for industry effluent water using PID controller. *Test Engineering and Management*, 82, 10733-10738. Retrieved from www.scopus.com
- [14] T. Arunkumari, V. Indra Gandhi, “A Review on Single Switch Dc-Dc Converter for Renewable Energy Based Applications”, International Conference on Innovations in Power and Advanced Computing Technologies, 2017.
- [15] Ouyang, Ziwei, et al. "Analysis and design of fully integrated planar magnetics for primary–parallel isolated boost converter." *IEEE Transactions on Industrial Electronics* 60.2 (2012): 494-508.
- [16] Goyal, V., & Deolia, V. K. (2020). Tuning of PID controller for paper machine headbox using hybrid PSOABC algorithm. *Test Engineering and Management*, 82(1-2), 1-11. Retrieved from www.scopus.com
- [17] T.Govindaraj, RasilaR,” Development of Fuzzy Logic Controller for DC-DCDC Buck Converters”, *International Journal of Engineering Techsci* Vol 2(2), 192-198, 2010.
- [18] Alanis, Alma Y., et al. "Real-time recurrent neural state estimation." *IEEE Transactions on Neural Networks* 22.3 (2011): 497-505.